Delignification's Effect on Microcrystalline Cellulose Obtained from Oil Palm Empty Fruit Bunch Fibres

Najieha Norazli,[a] Nurul Fazita Mohammad Rawi,[a,b,*] Owolabi Folahan Abdulwahab Taiwo,[c] Mohamad Haafiz Mohamad Kassim,[a,b,*] and Mohammad Jawaid [d]

The effects of acidified chlorite ($NaClO_2$) and totally chlorine free (TCF) bleaching were evaluated relative to the properties of microcrystalline cellulose (MCC) fabricated from oil palm empty fruit bunch fibres (OPEFB). The MCC properties were analyzed using X-ray diffraction (XRD), scanning electron microscopy (SEM), and thermogravimetric analysis (TGA) methods, and they were compared with commercial MCC. The results revealed that all MCC belongs to cellulose type 1 and OPEFB-$NaClO_2$-MCC showed a higher crystallinity index than OPEFB-TCF-MCC. The TGA indicated that all MCC samples showed a higher decomposition temperature compared to pure cellulose. However, OPEFB-$NaClO_2$-MCC showed better thermal stability than OPEFB-TCF-MCC. It was clear from SEM images that the different MCC particles had rough surfaces and micro-sized particles. Overall, results confirmed that the obtained MCC samples displayed comparable properties with those of commercial MCC. The MCC produced from OPEFB using $NaClO_2$ is a promising material to prepare high value-added products compared to MCC produced using TCF delignification treatment.

DOI: 10.15376/biores.18.1.1901-1915

Keywords: Oil palm empty fruit bunch; Microcrystalline cellulose; Acidified chlorite; Totally chlorine free; Structural properties; Thermal properties; Morphological properties

Contact information: a: Bioresource Technology Division, School of Industrial Technology, Universiti Sains Malaysia, Penang, Malaysia; b: Green Biopolymer, Coatings and Packaging Cluster, School of Industrial Technology, 11800 Minden Universiti Sains Malaysia; c: Pulp and Paper Division, Federal Institute of Industrial Research Oshodi, Lagos, Nigeria; d: Laboratory of Biocomposite Technology, INTROP, University Putra Malaysia, 43400 Serdang, Selangor, Malaysia;
** Corresponding authors: fazita@usm.my; mhaafiz@usm.my*

INTRODUCTION

The demand for sustainable and renewable materials has increased intensely in the last few decades and is the topic for the "2030 Agenda for Sustainable Development" organized by the United Nations General Assembly (2015). In line with the United Nations mantra "Transforming our world", the focus is to protect the planet from exploitation of its natural resources (Haldar and Purkait 2020). As awareness of the impact of climate change grows, researchers have reported that one of the most abundant and sustainable biopolymers on earth is cellulose. This versatile and renewable material can be obtained from various sources such as agricultural waste or biomass (Galiwango *et al.* 2019; Li *et al.* 2019; Mishra *et al.* 2019).

Natural cellulosic fibers derived from lignocellulosic biomass have several advantages, including their abundance, renewable nature, low cost, high specific strength, and reactive surfaces, coupled with their biocompatibility and biodegradability, which has

been a great asset in applying micro and nano-sized particles from cellulose fibre for enhancement of strength properties in composites. When compared to synthetic fibre composites, natural fibre composites use less energy to manufacture. Globally accessible natural fibres have been employed and studied as reinforcement in polymer composites such as bagasse (Alizadeh Asl *et al.* 2017; Abd El-Baky *et al.* 2019; Suresh *et al.* 2020), hemp (Dayo *et al.* 2017), and date palm (Awad *et al.* 2020; Alhijazi *et al.* 2020). These fibres offer similar qualities and can be used to replace synthetic fibre composites (Kannan and Thangaraju 2021). Since the production and report of microcrystalline cellulose (MCC) by Smith and Battista (1955), it has since been widely used in various industries because of its numerous advantages (Taiwo *et al.* 2016; Tarchoun *et al.* 2019). Any material that contains a high concentration of cellulose can be used to make MCC. Various lignocellulosic biomass sources for MCC are reported in the literature such as forest residue (rose stem and date seeds), agricultural residue (tea wastes), and aquatic residue (brown algae) (Haldar and Purkait 2020).

Malaysia's and the world's palm oil industries have continued to expand to sustainably meet the growing global demand for oils and fats as stated by the Malaysia palm oil council (2019). With a palm tree yielding only 10% oil, this growth results in a variety of wastes from oil palm products because of its vast planting lands and large number of oil palm mills (Shamsuddin *et al.* 2021). Oil palm activities generate a variety of wastes, including oil palm empty fruit bunches (OPEFB), oil palm fronds (OPF), and oil palm trunks (OPT) (Ramlee *et al.* 2021). This results in roughly 90% of enormous amounts of waste biomass from oil palm activities, while about 10% of oil extraction comes from two primary sources: plantations and mills. While oil palm plantations generate a large amount of oil palm trunks and fronds, other biomasses, such as mesocarp fibre, kernel shell, and empty fruit bunches are generated during the milling of fresh fruit bunches (Anuar *et al.* 2019). Oil palm empty fruit bunch generates up to 22 to 23 million tons of residue yearly in Malaysia and is the cheapest natural fibre with as good characteristics as a non-wood fibre. It has a lot of promising characteristics as a major raw material to replace woody plants, which are expensive in many sectors (Padzil *et al.* 2020). These organic and natural by-products have the potential to be employed as a value-added product in the industrial sector.

As with other plant species, cellulose, hemicellulose, and lignin are the major constituents of biomass' natural fibres, which also contain trace amounts of proteins and extractives. Cellulose is well-embedded in the intricate network of hemicellulose and lignin in each of the fibre materials. Apart from the treatment process chosen, the quality and quantity of cellulose used in the process dictate the formation of derivatives. Thus, it is critical to emphasize the structure and composition of cellulose within the lignocellulosic biomass fibres.

The properties of the modified cellulose properties are not only dependent on the type of lignocellulosic source but also on the pretreatments used to extract its native cellulose. These pretreatments are performed to separate pure and crystalline cellulose. They are also used to reduce the degree of polymerization and increase the reactivity of cellulose (Kargarzadeh *et al.* 2017). Due to the various factors that can affect the success of the pretreatment, it is important that the techniques are optimized to avoid generating toxic, hazardous wastes as well as high overall process costs (Phanthong *et al.* 2018). The delignification process is widely used to remove hemicellulose and lignin from raw biomass (Jiang and Hsieh 2015; Ilyas *et al.* 2018; Liao *et al.* 2020); however, various other methods have been used as well to remove hemicellulose and lignin. Asl, Mousavi, and

Labbafi (2017) extracted alpha cellulose using a digester at 370 °C, then bleached the fibres with chlorine gas and sodium hypochlorite. Asif *et al.* (2022) in other hands, delignified pedicles fiber with 5% wt NaOH solution and bleached the resulting fibres with sodium chlorite solution to obtain cellulose. Shi and Liu (2021) extracted cellulose using totally chlorine free bleaching method. The conventional method involves the use of chlorine-based protocol, but recent approaches are by green delignification with totally chlorine free methods (Cheng *et al.* 2018; Robles *et al.* 2018). To reduce the production of chlorinated organic compounds during pulp manufacturing, totally chlorine-free (TCF) bleaching is being used more frequently as a result of global trends and environmental pressures for cleaner bleaching processes (Li *et al.* 2017).

The dependence of the isolated pure cellulose and MCC from OPEFB on the raw material, the process, and also the pretreatments has been widely reported. Various previous studies have been conducted to generate MCC from OPEFB. Despite this, there have been no controlled studies comparing differences in the effects of pretreatment on the final characteristics of the derived MCC from OPEFB. This paper aims to improve the efficiency of the process by developing effective methods for the isolation and production of pure MCC from OPEFB and to compare two different pretreatment processes before MCC isolation. To achieve this, two delignification processes were employed in this study, the acidified chlorite ($NaClO_2$) method and the totally chlorine free (TCF) delignification method. The prepared MCC samples were characterized with analytical techniques of Fourier transform infrared (FT-IR), X-ray diffraction (XRD), scanning electron microscopy (SEM), and thermogravimetric analysis (TGA) to investigate the impact of the different delignification process used on the physiochemical and thermal properties of isolated MCC. The commercial MCC was used as reference to compare the properties of extracted MCC.

EXPERIMENTAL

Materials

The OPEFB strands were procured from United Oil Palm Sdn Bhd, Nibong Tebal, Penang, Malaysia. Commercial microcrystalline cellulose (Sigma-Aldrich (31069-7)) used as a control. Other materials used include distilled water, sodium hydroxide (NaOH), sodium chlorite ($NaClO_2$), acetic acid 98%, hydrochloric acid (HCl) 37%, magnesium sulphate heptahydrate ($MgSO_4.H_2O$), hydrogen peroxide (H_2O_2), sulphuric acid (H_2SO_4), ammonia hydroxide (NH_4OH), and silicon oil; all chemicals used were purchased from Sigma Aldrich, Merck (United States).

Preparation of OPEFB pulp with soda pulping

The OPEFB strands were pre-hydrolyzed *via* immersion in water for 1 h at 170 ℃ in a digester. The preparation of OPEFB pulp was completed by the pulping milieu as reported by Leh *et al*. (2008). After that, OPEFB was washed to eliminate all contaminations. A total of 300 g oven-dried (OD) OPEFB was pulped with 26% NaOH solution at a solid-to-liquid ratio of 1:7 and heated to 170 ℃ for 100 min. The obtained OPEFB pulp was then washed with water through a hydro pulper and then screened using pulp screening equipment with diameter of 15 mm. The fine OPEFB pulp was labeled as dissolving pulp and kept in the refrigerator for further study.

Preparation of totally chlorine-free cellulose

Three sequences that were used to produce totally chlorine-free (TCF) pulp include oxygen, ozone, and peroxide bleaching according to the procedure reported by Leh *et al.* (2008). Oxygen bleaching was completed using an autoclave equipped with a gas inlet, stirrer, and computer-controlled thermocouple manufactured by Parr Instrument Company, Moline, IL, USA. A total of 100 g OD of dissolved pulp was mixed with 1.0% magnesium sulfate ($MgSO_4.7H_2O$) solution, 2.0% sodium hydroxide (NaOH) solution, and an appropriate amount of water to achieve 10% concentration. The reaction temperature and oxygen pressure were maintained at 95 ℃ and 80 psi, respectively. The autoclave was maintained for 30 min with occasional stirring.

A modified revolving vessel designed for evaporation attached to an ozone generator and oxygen cylinder was used for ozone bleaching. The pulp was treated with acidic water at a pH of 1.5 (adjusted by addition of H_2SO_4) for 2 h. Then, the pulp was squeezed to a consistency of 27% and placed in a round bottom flask reaction vessel. The regenerated ozone gas was passed through the vessel and the vessel was rotated to make sure homogeneous mixing between pulp and ozone gas for 2.5 min. The reaction was continued for another 20 min. Then the obtained pulp was washed with distilled water.

The next stage was hydrogen peroxide bleaching, for which 3.0% hydrogen peroxide solution, 2.0% NaOH solution, and 0.5% $MgSO_4 \cdot 7H_2O$ solution based on pulp weight were mixed with an appropriate amount of water to achieve 15% concentration. The pulp slurry was transferred to a plastic bag and the reaction was completed at 65 ℃ for 1 h in a water bath and squeezed every 10 min to get proper extraction. The pulp was then treated with purified water. To obtain pure cellulose from delignified pulp, the pulp was then treated with 17.5% NaOH at 80 ℃ for 1 h following the Pachuau *et al*. (2014) method. The sample was filtered, repeatedly washed with distilled water to neutralize it, and oven-dried overnight at 40 ℃ and labeled as OPEFB-TCF-C.

Preparation of acidified sodium chlorite cellulose pulp

The dissolving pulp was added with acidified sodium chlorite according to the report by Foo *et al*. (2020). Then, 20 g of dissolving pulp was added with $NaClO_2$ and 10% of acetic acid until the pH reached 4. The dissolving pulp was boiled in sodium chlorite solution for 2 h at 80 ℃. The resultant delignified dissolving pulp was subsequently washed with distilled water. To obtain pure cellulose from delignified pulp, the pulp was treated with 17.5% NaOH at 80 ℃ for 1 h following Pachuau *et al*.'s (2014) method. The sample was filtered, repeatedly washed with distilled water to neutralize it and oven-dried overnight at 40 ℃ and denoted as OPEFB-$NaClO_2$-C.

Production of OPEFB MCC

The acid hydrolysis treatment was conducted to obtain MCC according to the optimized method describe by Hassan *et al.* (2019). 10 g oven dried weight of OPEFB cellulose sample was added with 2.5 N hydrochloric acid with the ratio of 1:20 (OPEFB cellulose to dilute acid) and heated using silicon oil at temperature 106 °C for 20 min. After being hydrolyzed, the sample was then washed with distilled water and 5% NH_4OH solution to achieve a neutral pH of 7. The sample was then dried at 40 ℃ overnight until consistent weight and subsequently ground into fine powder.

Methods

Fourier transform infrared spectroscopy

Fourier transform infrared spectroscopy was performed on an infrared spectrometer (Perkin-Elmer; PC1600, USA) using the potassium bromide (KBr) method. The oven-dried powder of each sample was mixed with KBr with a ratio of 1:100 and then pressed to form a pellet. The pellet was scanned within the range of 500 to 4000 cm^{-1} at a resolution of 4 cm^{-1}.

Thermogravimetric analysis

A thermogravimetric analyzer (TGA/DSC 1; Mettler-Toledo, Switzerland) was used to determine the thermal stability of the samples. The samples were scanned from 30 °C to 800 °C at a rate of 10 °C/min^{-1} under a nitrogen gas atmosphere. The thermograms showed the plot of weight loss percentage against the temperature.

Differential scanning calorimetry

To determine the melting temperature for all samples, a modified Perkin Elmer Pyris 7 thermal analyzer was used under nitrogen purge at a heating rate of 10 °C/min from room temperature to 400 °C.

Morphological analysis

The morphological characteristics of the samples were observed using SEM analysis (Leo Supra 50 VP Field Emission; Carl- ZEISS SMT, Oberkochen, Germany). The entire sample was dried overnight in an oven at 40 °C to remove moisture. Then, the sample was coated with platinum before imaging to avoid charging.

X-ray diffraction analysis

The crystallinity of all samples was determined using XRD (D8 Advance; Bruker, Germany), and diffractograms of all samples were collected. The sample data crystallinity was obtained at 2θ between 5° and 45°. The approach of Segal *et al.* (1959) was used to measure the degree of crystallinity index using Equation 1 as follows,

$$\text{CrI}\ (\%) = (I_{200} - I_{am}) / I_{200} \times 100 \quad (1)$$

where I_{200} is the peak intensity of the crystalline fraction and I_{am} is the peak intensity of the amorphous fraction.

RESULTS AND DISCUSSION

FT-IR Analysis

The FT-IR spectra of OPEFB-Raw, OPEFB-Unbleached Pulp, OPEFB-$NaClO_2$-C, OPEFB-TCF-C, OPEFB-$NaClO_2$-MCC, and OPEFB-TCF-MCC obtained are presented in Fig. 1. The peak assignments are summarized in Table 1. Based on Fig. 1, all samples showed three main absorbance regions, which are single bond region (2500 to 4000 cm^{-1}), double bond region (1500 to 2000 cm^{-1}), and fingerprint region (600 to 1500 cm^{-1}) (Nandiyanto *et al.* 2019). There are more than five absorbance bands, indicating that the sample is a complex molecule.

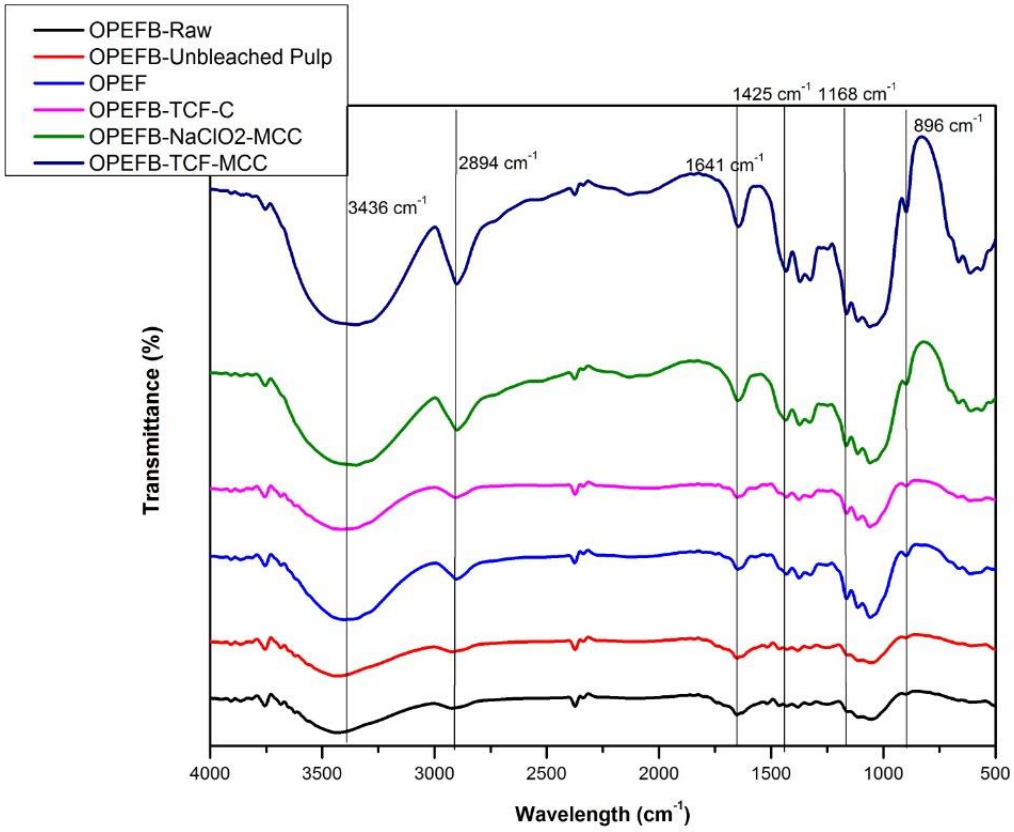

Fig. 1. FT-IR spectra of OPEFB-Raw, OPEFB-Unbleached Pulp, OPEFB-$NaClO_2$-C, OPEFB-TCF-C, OPEFB-$NaClO_2$-MCC, and OPEFB-TCF-MCC

There was a broad peak in the range 3200 to 3600 cm^{-1}, indicating a hydrogen bond. This band confirms the presence of hydrate (H_2O) and hydroxyl (OH) groups. The broad peak located from 3200 to 3600 cm^{-1} was assigned to the stretching vibration of -OH groups while the peak at 2900 cm^{1} represented the stretching vibration of C-H in -CH_2 groups of primary alcohol (Fathy *et al.* 2016). In the double bond region (1500 to 2000 cm^{-1}), peaks at 1641 cm^{-1} were detected. The absorbance band at 1641 cm^{-1} was due to the O-H bending of water molecules, and this showed the absorbance of water molecules by the samples due to the strong interaction between water molecules and cellulose (Haafiz *et al.* 2013; Trache *et al.* 2016). In the fingerprint region (600 to 1500 cm^{-1}), several peaks were detected and indicated an aromatic ring. The absorbance band at 1425 cm^{-1} was assigned to the bending vibration of -CH_2 group (Haafiz *et al*. 2013). The absorbance band at 1168 cm^{-1} was due to the stretching vibration of a glycosidic bond (C-O-C), while the absorbance band at 896 cm^{-1} attributed to the rock vibration of C-H in cellulose (Fahma *et al.* 2010; Haafiz *et al.* 2013). From Fig. 1, the absorbance band at 1518 cm^{-1} can be seen clearly in the EFB spectrum and was due to the skeletal vibration of aromatic C=C. However, the absorbance band was absent in the spectra of bleached pulp ($NaClO_2$-Pulp and TCF-Pulp) and MCC from both OPEFB-$NaClO_2$-MCC and OPEFB-TCF-MCC, indicating that the lignin component in the EFB sample was completely removed after bleaching (Fahma *et al.* 2010; Haafiz *et al*. 2013). Moreover, the intensity of the peak at 1433 cm^{-1} for OPEFB-TCF-MCC increased, which suggested a higher degree of crystallinity of OPEFB-TCF-MCC (Hussin *et al.* 2016).

Table 1. FT-IR Spectral Peak Assignments for OPEFB-Raw, OPEFB-Unbleached Pulp, OPEFB-$NaClO_2$-C, OPEFB-TCF-C, OPEFB-$NaClO_2$-MCC, and OPEFB-TCF-MCC

Sample Wavenumber (cm^{-1})	Peak Assignment
3200 to 3600	O-H stretching
2894	-CH_2 group stretching
1641	O-H bending
1425	Bending of -CH_2 group
1168	C-O-C stretching
896	C-H rock vibration

Through comparing the FT-IR spectra obtained, the spectra did not show particular changes based on the peak frequency, which suggested that the acid hydrolysis used to produce the MCC from bleached pulp will not affect the chemical structure of cellulosic components in MCC (Haafiz *et al.* 2013, 2014)

Thermal Properties

The results of the thermogravimetric analysis TGA (Fig. 2a) and differential thermogravimetric analysis DTG (Fig. b) curves were used to characterize the chemical phase to ascertain the thermal stability of cellulose and MCCs samples (OPEFB-Raw, OPEFB-Unbleached Pulp, OPEFB-$NaClO_2$-C, OPEFB-TCF-C, OPEFB-$NaClO_2$-MCC, OPEFB-TCF-MCC). Table 2 shows the summary of the result of the changes in the thermal properties of the prepared samples which is important for the development of high temperature biocomposite materials.

Table 2. Thermal Properties of OPEFB-Raw, OPEFB-Unbleached Pulp, OPEFB-$NaClO_2$-C, OPEFB-TCF-C, OPEFB-$NaClO_2$-MCC, and OPEFB-TCF-MCC

Samples	Onset Temperature	Residual Weight (%) at 400 (°C)	DTG Peak Temperature, T_{max} (°C)
OPEFB-Raw	293.18	30.28	343
OPEFB-Unbleached Pulp	341.74	2.3	366
OPEFB-$NaClO_2$-C	326.91	14.28	359
OPEFB-TCF-C	333.03	10.26	352
OPEFB-$NaClO_2$-MCC	325.44	13.74	343
OPEFB-TCF-MCC	307.51	11.22	327

The TGA graph illustrated the sample's weight loss over time while it was heated at a constant ramp rate. In the range of 50 to 400 °C, the thermogram curve revealed two weight loss expressions. Based on Fig. 2, the initial weight loss in the range of 50 to 150 °C was due to the evaporation of water from the surface of the samples. The sample's intermolecular hydrogen bound water was evaporated at a temperature of around 150 °C. The second set of decreased in the curves in the range of 250 to 400 °C was due to the degradation of cellulose *via* disintegration of glycosyl units followed by transformation to char that occurred at maximum temperature of 250 °C to 400 °C, accounting for around 80% of the overall degradation. This was followed by the char formation (Haafiz *et al.* 2013, 2019).

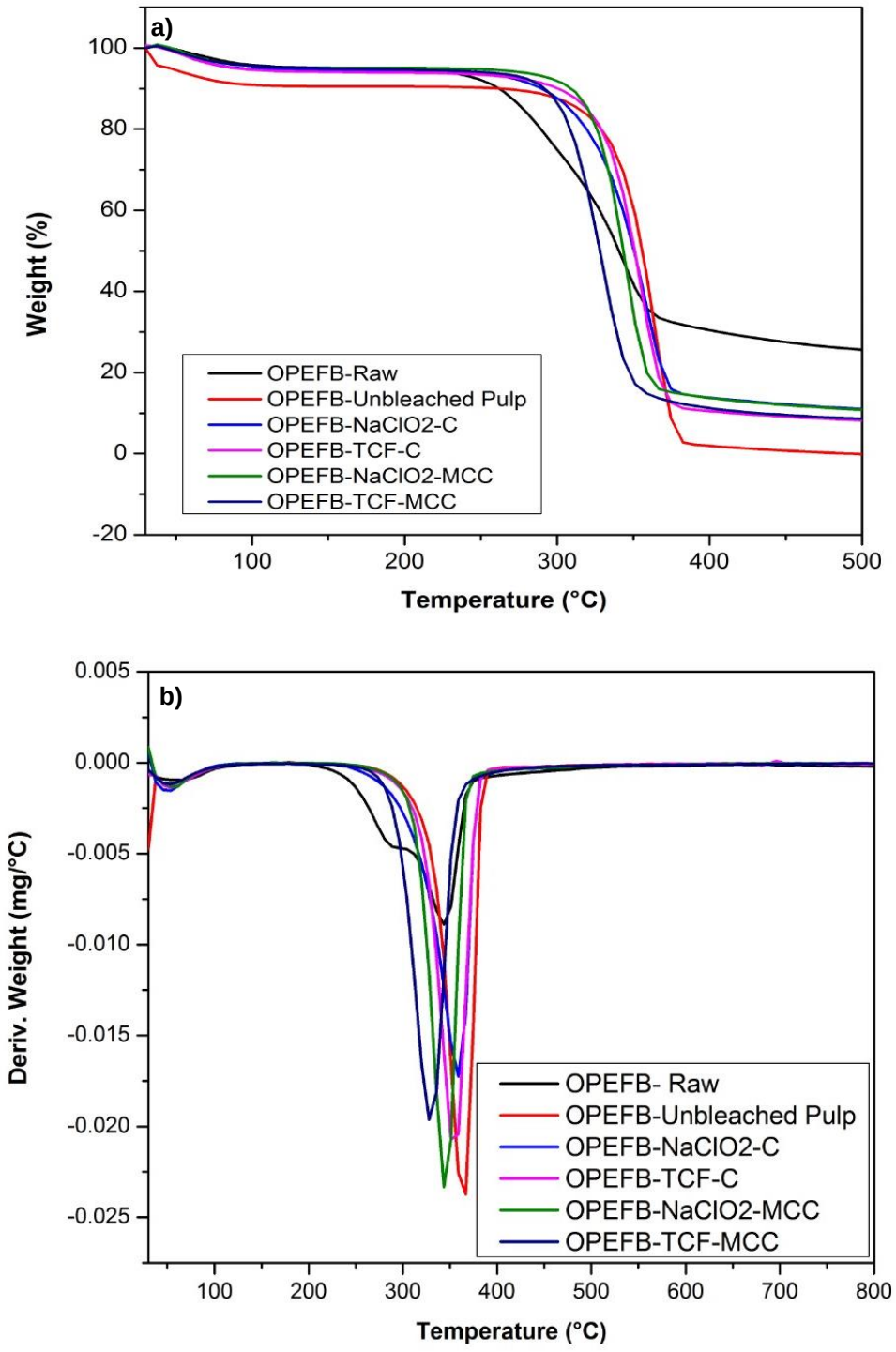

Fig. 2. a) TGA and b) DTG curves of OPEFB-Raw, OPEFB-Unbleached Pulp, OPEFB-$NaClO_2$-C, OPEFB-TCF-C, OPEFB-$NaClO_2$-MCC, and OPEFB-TCF-MCC

Thermal degradation was seen at a lower temperature than the cellulose sample throughout a wider temperature range, indicating a reduced thermal stability because of a higher number of free ends in the chain, a reduction in molecular weight, and breakdown of cellulose's amorphous domains (Mandal and Chakrabarty 2011). This result was similar with previous studies (Haafiz *et al.* 2013; Hassan *et al.* 2019).

Based on Table 2, the degradation and DTG peak temperature of MCC were lower than OPEFB cellulose pulp, which may be due to the drastic decrease in the molecular weight of the latter caused by the acid hydrolysis that makes it more vulnerable to degrade when temperature increases (Haafiz *et al.* 2013; Dungani *et al.* 2017). It was observed that sample that was prepared using $NaClO_2$ treatment displayed higher thermal stability compared to those obtained by the TCF treatment.

However, the residual weight of MCC at 400 °C was higher than that of cellulose pulp due to the high crystallinity of MCC that makes it more flame resistant (Mandal and Chakrabarty 2011; Haafiz *et al.* 2013). Furthermore, it is worth mentioning that the sample prepared using $NaClO_2$ delignification showed higher residual weight at 400 °C compared to those obtained by TCF treatment. The highest residual weight of EFB at 400 °C suggested that it contains inorganic material, such as ash, that cannot be degraded during the analysis (Taiwo *et al.* 2017).

Morphology Analysis

The surface morphology of all the OPEFB cellulose and MCC samples was also studied by SEM analysis, as shown in Fig. 3 (a to f). It was discovered that the morphology of MCC changed after treatment. The SEM images showed changes of morphology dimensions in terms of size and shapes of OPEFB pulp and OPEFB MCC.

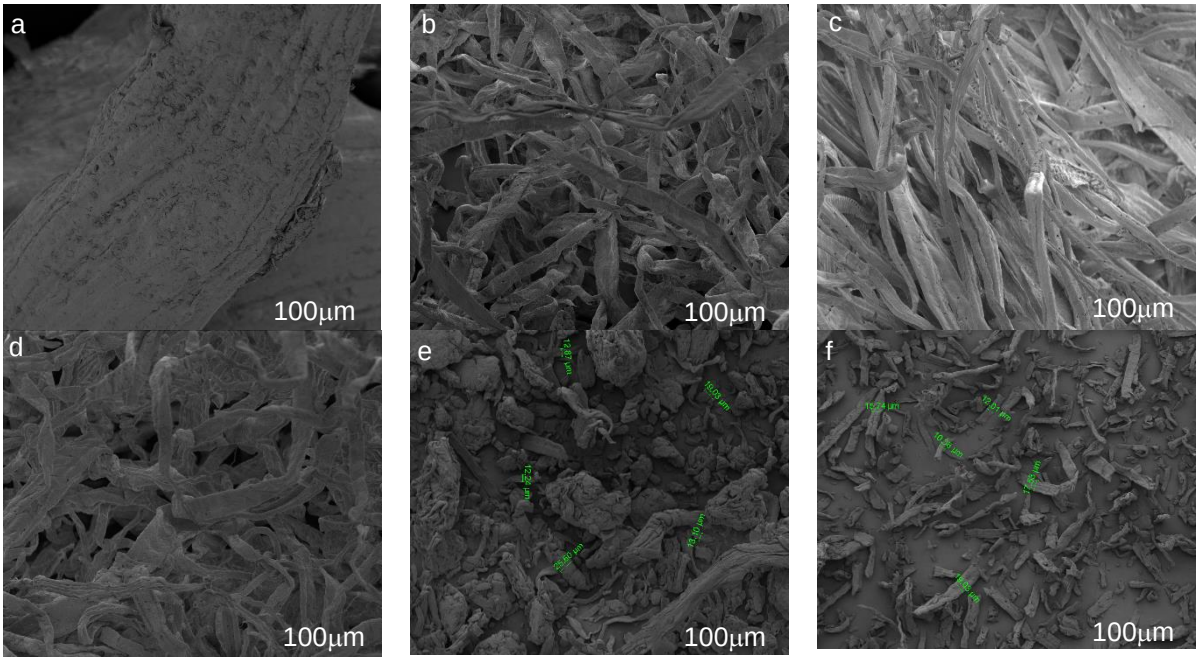

Fig. 3. SEM images of all cellulose: a) OPEFB-Raw, b) OPEFB-Unbleached Pulp, c) OPEFB-NaClO2-C, d) OPEFB-TCF-C, e) OPEFB-NaClO2-MCC, and f) OPEFB-TCF-MCC

The OPEFB-Raw as Fig. 3a shows a slightly rough surface area with irregular flake-like structure, which possibly can be attributed to the presence of substances like wax, lignin, and hemicelluloses (Taiwo et *al.* 2017). After alkaline treatment without delignification process, there was no noticeable different between OPEFB- Raw and OPEFB-Unbleached Pulp. Bleaching treatment clearly changed the morphology of the OPEFB as shown in Figs. 3c and 3d. Both $NaClO_2$ and TCF bleached samples showed a clean and smoother surface and showed a long and uniform fibre. This result indicated that lignin and hemicelluloses were removed.

The MCC obtained after acid hydrolysis of the all the cellulose exhibited irregular shape, small-sized fibrils with diameters ranging from 10 to 19 μm, and the MCC also agglomerated with each other. Each bleaching treatment shows a slightly rough surface. Because of depolymerisation of cellulose polymers to a shorter chained MCC, the structure of MCC differed from that of cellulose (Mat Soom *et.al.* 2009).This was probably caused by removal of hemicellulose, silica, and lignin.

XRD Analysis

X-Ray diffraction analysis was used to study the crystallographic structure of prepared sample materials. The XRD pattern of OPEFB-Raw, OPEFB-Unbleached Pulp, OPEFB-$NaClO_2$-C, OPEFB-TCF-C, OPEFB-$NaClO_2$-MCC, and OPEFB-TCF-MCC are presented in Fig. 4. The patterns of XRD of various fibres are shown in Fig. 4. The peaks of these fibres were associated with cellulose type I structure.

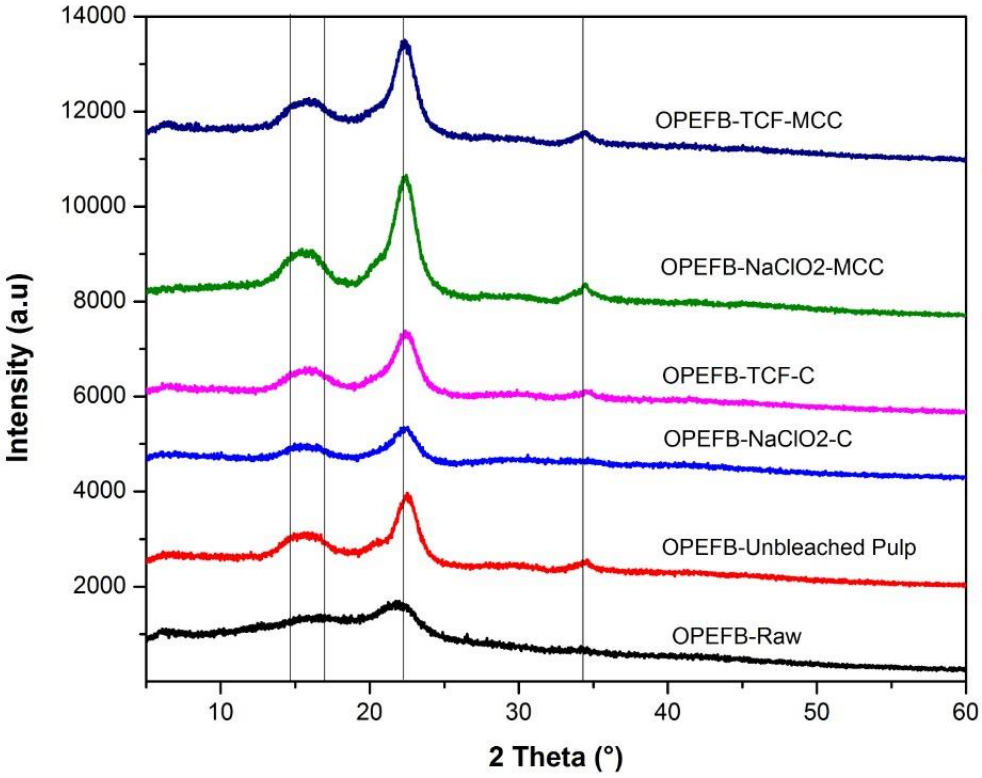

Fig. 4. XRD pattern of OPEFB-Raw, OPEFB-Unbleached Pulp, OPEFB-$NaClO_2$-C, OPEFB-TCF-C, OPEFB-$NaClO_2$-MCC, and OPEFB-TCF-MCC

The percentage of crystallinity index, CI (%), of all samples was calculated and displayed in Table 3. Studies show that cellulose consists of both crystalline and amorphous regions. Based on literature studies, the structure of the samples showed four characteristic peaks, with amplitudes ranging from 14 to 34.4. It is clear that cellulose I does not have doublets and that the absence of cellulose II is observable. Analysis showed that the crystallinity index of the MCC sample was higher than the starting cellulose sample. This indicates the removal of amorphous regions throughout the process. In this study, the crystallinity index of MCC from $NaClO_2$ delignification method compared to MCC from TCF delignification was 64.5% and 61.5%, respectively. The MCC with $NaClO_2$ delignification method showed the peaks as sharper and more intense as compared to the TCF delignification method. This might be due to the presence of some hemicelluloses that are not completely removed in TCF delignification, which leads to selective solubilization of the amorphous and hemicelluloses rather than the amorphous part of cellulose (Kishani *et al.* 2018).

Table 3. CI of OPEFB-Raw, OPEFB-Unbleached Pulp, OPEFB-$NaClO_2$-C, OPEFB-TCF-C, OPEFB-NaClO2-MCC, and OPEFB-TCF-MCC

Sample	Crystallinity Index (%)
OPEFB-Raw	52.99
OPEFB-Unbleached Pulp	60.24
OPEFB–$NaClO_2$-C	60.07
OPEFB-TCF-C	59.85
OPEFB-$NaClO_2$- MCC	64.48
OPEFB-TCF-MCC	61.51

This result further shows that the acid hydrolysis process is not only utilized to hydrolyze the amorphous portions of cellulose molecules, but it also removes the remaining amorphous hemicelluloses.

CONCLUSIONS

1. Microcrystalline cellulose (MCC) was successfully isolated from oil palm empty fruit bunch (OPEFB) using different delignification processes after the acid hydrolysis process. The study showed a notable effect of the diversified delignification protocols on the MCC samples based on the characterization, studies of both MCC produced were comparable to commercial MCC-CMCC.
2. The scanning electron microscopy (SEM) analysis illustrated that $NaClO_2$ - MCC exhibited a rough and compact structure, similar to TCF-MCC, although it exhibited smaller size of MCC. The Fourier transform infrared (FTIR) analysis revealed that both acidified chlorite and totally chlorine free (TCF) delignification influenced the purity of cellulose without any impact on cellulose chemical structure. The X-ray diffraction (XRD) analysis showed that the different delignification methods used did not alter the crystal structure from the cellulose 1 allomorph of OPEFB, and the crystallinity index ranged from 61% to 69%. From the studies, acidified chlorite delignification produced a higher crystallinity index of MCC than the MCC produced from TCF delignification. Thermal analysis indicated that MCC produced through acidified chlorite delignification cellulose had good thermal stability compared to TCF delignification.

3. The finding of this study suggests that OPEFB MCC prepared with acidified chlorite delignification presented higher crystallinity index and higher thermal stability compared to TCF delignification process. However, the scope of these studies does not cover environmental considerations; it is only limited to diverse preparation milieu.
4. The study concludes that MCC samples produced from OPEFB using $NaClO_2$ is capable of giving high-value composite products compared to the MCC produced using TCF delignification treatment.

ACKNOWLEDGMENTS

The authors acknowledge Fundamental Research Grant Scheme (Grant number: FRGS/1/2022/STG05/USM/02/10), for providing financial support for this research.

REFERENCES CITED

Abd El-Baky, M. A., Megahed, M., El-Saqqa, H. H., and Alshorbagy, A. E. (2019). "Mechanical properties evaluation of sugarcane bagasse-glass/ polyester composites," *Journal of Natural Fibers* 18(8), 1163-1180. DOI:10.1080/15440478.2019.1687069

Alhijazi, M., Zeeshan, Q., Safaei, B., Asmael, M., and Qin, Z. (2020). Recent developments in palm fibers composites: A Review. *Journal of Polymers and the Environment* 28(12), 3029–3054. DOI: 10.1007/s10924-020-01842-4

Alizadeh Asl, S., Mousavi, M., and Labbafi, M. (2017). Synthesis and characterization of carboxymethyl cellulose from sugarcane bagasse. *Journal of Food Processing & Technology* 08(08). DOI: 10.4172/2157-7110.1000687

Anuar, N. I. S., Zakaria, S., Gan, S., Chia, C. H., Wang, C., and Harun, J. (2019). "Comparison of the morphological and mechanical properties of oil palm EFB fibres and kenaf fibres in nonwoven reinforced composites," *Industrial Crops and Products* 127, 55-65. DOI: 10.1016/j.indcrop.2018.09.056

Asif, M., Ahmed, D., Ahmad, N., Qamar, M. T., Alruwaili, N. K., and Bukhari, S. N. (2022). "Extraction and characterization of microcrystalline cellulose from *Lagenaria siceraria* fruit pedicles," *Polymers* 14(9), 1867. DOI: 10.3390/polym14091867

Awad, S., Zhou, Y., Katsou, E., Li, Y., and Fan, M. (2020). "A critical review on date palm tree (*Phoenix dactylifera* L.) fibres and their uses in bio-composites," *Waste and Biomass Valorization* 12(6), 2853-2887. DOI: 10.1007/s12649-020-01105-2

Cheng, F., Zhao, X., and Hu, Y. (2018). "Lignocellulosic biomass delignification using aqueous alcohol solutions with the catalysis of acidic ionic liquids: A comparison study of solvents," *Bioresource Technology* 249, 969-975. DOI: 10.1016/j.biortech.2017.10.089

Dayo, A. Q., Gao, B.-C., Wang, J., Liu, W.-B., Derradji, M., Shah, A. H., and Babar, A. A. (2017). "Natural hemp fiber reinforced polybenzoxazine composites: Curing behavior, mechanical and thermal properties," *Composites Science and Technology* 144, 114-124. DOI: 10.1016/j.compscitech.2017.03.024

Dungani, R., Taiwo, O. F. A., Saurabh, C. K., Khalil, H. P. S. A., Tahir, P. M., Hazwan, C. I. C. M., Ajijolakewu, K. A., Masri, M. M., Rosamah, E., and Aditiawati, P. (2017). "Preparation and fundamental characterization of cellulose nanocrystal from

oil palm fronds biomass," *Journal of Polymers and the Environment* 25, 692-700. DOI: 10.1007/s10924-016-0854-8

Fahma, F., Iwamoto, S., Hori, N., Iwata, T., and Takemura, A. (2010). "Isolation, preparation, and characterization of nanofibres from oil palm empty-fruit-bunch (OPEFB)," *Cellulose* 17(5), 977-985. DOI: 10.1007/s10570-010-9436-4

Fathy, M., Moghny, T. A., Mousa, M. A., El-Bellihi, A.-H. A.-A., and Awadallah, A. E. (2016). "Absorption of calcium ions on oxidized graphene sheets and study its dynamic behavior by kinetic and isothermal models," *Applied Nanoscience* 6(8), 1105-1117. DOI: 10.1007/s13204-016-0537-8

Foo, M. L., Ooi, C. W., Tan, K. W., and Chew, I. M. (2020). "A step closer to sustainable industrial production: Tailor the properties of nanocrystalline cellulose from oil palm empty fruit bunch." *Journal of Environmental Chemical Engineering* 8(5), article 104058. DOI: 10.1016/j.jece.2020.104058

Galiwango, E., Rahman, N. S. A., Marzouqi, A. H. A., Omar, M. M. A., and Khaleel, A.A. (2019). "Isolation and characterization of cellulose and α-cellulose from date palm biomass waste." *Heliyon* 5(12). DOI: 10.1016/j.heliyon.2019.e02937

"General Assembly: UN Transforming our world: The 2030 agenda for sustainable development" (2015). (https://sustainabledevelopment.un.org/post2015/transformingourworld), Accessed 03 June 2021

Haafiz, M. K. M., Eichhorn, S. J., Hassan, A., and Jawaid, M. (2013). "Isolation and characterization of microcrystalline cellulose from oil palm biomass residue," *Carbohydrate Polymers* 93(2), 628-634. DOI: 10.1016/j.carbpol.2013.01.035

Haafiz, M. K. M., Hassan, A., Zakaria, Z., and Inuwa, I. M. (2014). "Isolation and characterization of cellulose nanowhiskers from oil palm biomass microcrystalline cellulose," *Carbohydrate Polymers* 103, 119-125. DOI: 10.1016/j.carbpol.2013.11.055

Haafiz, M. K. M., Taiwo, O. F. A., Razak, N., Hashim, R., Hussin M. H., and Rawi, N. F. M. (2019). "Development of green MMT-modified hemicelluloses based nanocomposite film with enhanced functional and barrier properties," *BioResources* 14(4), 8029-8047. DOI: 10.15376/biores.14.4.8029-8047

Haldar, D., and Purkait, M. K. (2020). "Micro and nanocrystalline cellulose derivatives of lignocellulosic biomass: A review on synthesis, applications and advancements," *Carbohydrate Polymers* 250, article 116937. DOI: 10.1016/j.carbpol.2020.116937

Hassan, T. M., Hossain, M. S., Kassim, M. H., Ibrahim, M., Rawi, N. F. M., and Hussin, M. H. (2019). "Optimizing the acid hydrolysis process for the isolation of microcrystalline cellulose from oil palm empty fruit bunches using response surface methods," *Waste and Biomass Valorization* 11(6), 2755-2770. DOI: 10.1007/s12649-019-00627-8

Hussin, M. H., Pohan, N. A., Garba, Z. N., Kassim, M. J., Rahim, A. A., Brosse, N., Yemloul, M., Fazita, M. R. N., and Haafiz, M. K. M. (2016). "Physicochemical of microcrystalline cellulose from oil palm fronds as potential methylene blue adsorbents," *InternationalJournal of Biological Macromolecules* 92, 11-19. DOI: 10.1016/j.ijbiomac.2016.06.094

Ilyas, R. A., Sapuan, S. M., and Ishak, M. R. (2018). "Isolation and characterization of nanocrystalline cellulose from sugar palm fibres (*Arenga pinnata*)," *Carbohydrate Polymers* 181, 1038-1051. DOI: 10.1016/j.carbpol.2017.11.045

Jiang, F., and Hsieh, Y. L. (2015). "Cellulose nanocrystal isolation from tomato peels and assembled nanofibers," *Carbohydrate Polymers* 122, 60-68. DOI: 10.1016/j.carbpol.2014.12.064

Kannan, G., and Thangaraju, R. (2021). "Recent progress on natural lignocellulosic fiber reinforced polymer composites: A Review," *Journal of Natural Fibers* 19, 7100-7131. DOI: 10.1080/15440478.2021.1944425

Kargarzadeh, H., Ahmad, I., Thomas, S., and Dufresne, A. (2017). *Handbook of Nanocellulose and Cellulose Nanocomposites*, Wiley-VCH Verlag GmbH & Co.

Kishani, S., Vilaplana, F., Xu, W., Xu, C., and Wågberg, L. (2018). "Solubility of softwood hemicelluloses," *Biomacromolecules* 19(4), 1245-1255. DOI: 10.1021/acs.biomac.8b00088

Leh, C. P., Rosli, W. D. W., Zainuddin, Z., and Tanaka, R. (2008). "Optimisation of oxygen delignification in production of totally chlorine-free cellulose pulps from oil palm empty fruit bunch fibre," *Industrial Crops and Products* 28(3), 260-267. DOI: 10.1016/j.indcrop.2008.02.016

Liao, J. J., Latif, N. H., Trache, D., Brosse, N., and Hussin, M. H. (2020). "Current advancement on the isolation, characterization and application of lignin," *International Journal of Biological Macromolecules* 162, 985-1024. DOI: 10.1016/j.ijbiomac.2020.06.168

Li, P., Hou, Q., Zhang, M., and Li, X. (2017). "Environmentally friendly bleaching on bamboo (*Neosinocalamus*) kraft pulp cooked by displacement digester system," *BioResources* 13(1). DOI: 10.15376/biores.13.1.450-461

Li, S., Deng, W., Li, Y., Zhang, Q., and Wang, Y. (2019). "Catalytic conversion of cellulose based biomass and glycerol to lactic acid," *Journal of Energy Chemistry* 32, 138-151. DOI: 10.1016/j.jechem.2018.07.012

Malaysian palm oil industry. Malaysian Palm Oil Council. (2019). Retrieved February 22, 2022, from (https://mpoc.org.my/malaysian-palm-oil-industry/)

Mandal, A., and Chakrabarty, D. (2011). "Isolation of nanocellulose from waste sugarcane bagasse (scb) and its characterization," *Carbohydrate Polymers* 86(3), 1291-1299. DOI: 10.1016/j.carbpol.2011.06.030

Mat Soom, R., Abd Aziz, A., Wan Hassan, W. H., and Md Top, A. G. (2009). "Solid-state characteristics of microcrystalline cellulose from oil palm empty fruit bunch fibre," *Journal of Oil Palm Research* 21, 613-620.

Mishra, S., Kharkar, P. S., and Pethe, A. M. (2019). "Biomass and waste materials as potential sources of nanocrystalline cellulose: Comparative review of preparation methods," *Carbohydrate Polymers* 207, 418-427. DOI: 10.1016/j.carbpol.2018.12.004

Nandiyanto, A. B., Oktiani, R., and Ragadhita, R. (2019). "How to read and interpret FTIR spectroscope of organic material," *Indonesian Journal of Science and Technology* 4(1), 97. DOI: 10.17509/ijost.v4i1.15806

Pachuau, L., Lalhlenmawia, H., Tripathi, S. K., and Vanlalfakawma, D. C. (2014). "Muli bamboo (*Melocanna baccifera*) as a new source of microcrystalline cellulose," *Journal of Applied Pharmaceutical Science* 4(11), 87-94. DOI: 10.7324/japs.2014.41115

Padzil, F. N., Lee, S. H., Ainun, Z. M., Lee, C. H., and Abdullah, L. C. (2020). "Potential of oil palm empty fruit bunch resources in nanocellulose hydrogel production for versatile applications: A review," *Materials* 13(5), 1245. DOI: 10.3390/ma13051245

Phanthong, P., Reubroycharoen, P., Hao, X., Xu, G., Abudula, A., and Guan, G. (2018). "Nanocellulose: Extraction and application," *Carbon Resources Conversion* 1(1), 32-43. DOI: 10.1016/j.crcon.2018.05.004

Ramlee, N. A., Naveen, J., and Jawaid, M. (2021). "Potential of oil palm empty fruit bunch (OPEFB) and sugarcane bagasse fibres for thermal insulation application – A review," *Construction and Building Materials* 271, article 121519. DOI: 10.1016/j.conbuildmat.2020.121519

Robles, E., Fernández-Rodríguez, J., Barbosa, A. M., Gordobil, O., Carreño, N. L. V., and Labidi, J. (2018). "Production of cellulose nanoparticles from blue agave waste treated with environmentally friendly processes," *Carbohydrate Polymers* 183, 294-302. DOI: 10.1016/j.carbpol.2018.01.015

Segal, L., Creely, J. J., Martin, A. E., and Conrad, C. M. (1959). "An empirical method for estimating the degree of crystallinity of native cellulose using the x-ray diffractometer," *Textile Research Journal* 29(10), 786-794. DOI: 10.1177/004051755902901003

Shamsuddin, R., Singh, G., Kok, H. Y., Rosli, M. H., Cahyono, N. A. D., Lam, M. K., Lim, J. W., and Low, A. (2021). "Palm oil industry—processes, by-product treatment and value addition," *Sustainable Bioconversion of Waste to Value Added Products* 2021, 121-143. DOI: 10.1007/978-3-030-61837-7_8

Shi, S.-C., and Liu, G.-T. (2021). "Cellulose nanocrystal extraction from rice straw using a chlorine-free bleaching process," *Cellulose* 28, 6147-6158. DOI: 10.1007/s10570-021-03889-5

Suresh, S., Sudhakara, D., and Vinod, B. (2020). "Investigation on industrial waste eco-friendly natural fiber-reinforced polymer composites," *Journal of Bio- and Tribo-Corrosion* 6(2). DOI: 10.1007/s40735-020-00339-w

Taiwo, O. F. A., Haafiz M. K. M., Hossain M. S., and Rawi, N.F. M. (2016). "Influence of alkaline hydrogen peroxide pre-hydrolysis on the isolation of microcrystalline cellulose from oil palm fronds," *International Journal of Biological Macromolecules* 1-7. DOI: 10.1016/j.ijbiomac.2016.11.016

Taiwo, O. F. A., Saurabh, C. K., Dungani, R., and Khalil, H. P. S. A. (2017). "Spectroscopy and microscopy of microfibrillar and nanofibrillar composites," in: *Micro and Nano Fibrillar Composites (MFCs and NFCs) from Polymer Blends*, pp. 279-299. DOI:10.1016/B978-0-08-101991-7.00012-1

Tarchoun, A. F., Trache, D., and Klapötke, T. M. (2019). "Microcrystalline cellulose from Posidonia oceanica brown algae: Extraction and characterization," *International Journal of Biological Macromolecules* 138, 837-845. DOI: 10.1016/j.ijbiomac.2019.07.176

Trache, D., Hussin, M. H., Chuin, C. T. H., Sabar, S., Nurul Fazita, M. R., Taiwo, O. F. A., Hassan, T. M., and Haafiz, M. K. M. (2016). "Microcrystalline cellulose: Isolation, characterization and bio-composites application − A review," *International Journal of Biological Macromolecules* 93(Pt A), 789-804. DOI: 10.1016/j.ijbiomac.2016.09.056

Article submitted: June 1, 2022; Peer review completed: August 28, 2022; Revised version received: October 21, 2022; Accepted: December 19, 2022; Published: January 20, 2023.
DOI: 10.15376/biores.18.1.1901-1915